Velocity Measurement Techniques for Liquid Metal Flows

Sven Eckert, Andreas Cramer, and Gunter Gerbeth

Forschungszentrum Rossendorf, P.O.Box 510119, 01314 Dresden, Germany
(s.eckert@fz-rossendorf.de)

1 Introduction

Analysis and control of fluid flows, often subsidiary to industrial design issues, require measurements of the flow field. For classical transparent fluids such as water or gas a variety of well-developed techniques (laser Doppler and particle image velocimetry, Schlieren optics, interferometric techniques, etc.) have been established. In contrast, the situation regarding opaque liquids still lacks almost any commercial availability. Metallic and semiconductor melts often pose additional problems of high temperature and chemical aggressiveness, rendering any reliable determination of the flow field a challenging task. This review intends to summarise different approaches suitable for velocity measurements in liquid metal flows and to discuss perspectives, particularly in view of some recent developments (ultrasound, magnetic tomography). Focusing mainly on local velocity measurements, it is subsequently distinguished between invasive and non-invasive methods, leaving entirely aside the acquisition of temperature, pressure, and concentration, for which [1] may serve as a comprehensive reference.

2 Invasive techniques

In this context, invasiveness means insertion of a sensing unit into the medium under investigation, the consequence of which is twofold. We are not mainly concerned with probably adverse effects on the sensor owing to, e.g., high temperature or chemical aggressiveness, which ultimately boils down to a question of material science, rather than with the influence of the probe on the flow. This potential disturbance determines, besides their functional principles, the applicability of various types of anemometers to a considerable extent. On this note, different sensors are at first described and then discussed with particular attention to sensitivity.

S. Molokov et al. (eds.), Magnetohydrodynamics – Historical Evolution and Trends, 275–294.

Velocity probes to be immersed into the fluid can be classified, according to the underlying physical effect, into force reaction, thermal, and conductive sensors. Note that neither this small list is downright complete nor is it possible to review all variants in each category due to the scope of this review. Following history, we start with the force reaction probes, because these had been the first employed in order to determine velocities in moving fluids.

2.1 Force reaction probes

These probes respond to the force exerted onto them by the flowing medium, which is in principle a pressure. Presumably, the best-known mechanical anemometer is the vane type used in weather stations in order to determine wind speed. It usually consists of a few hemispheres or cups attached to radial spokes. The rotation speed can be measured by a number of different mechanisms. Often a magnet, affixed to the shaft, traversing past a fixed coil induces a pulse for each revolution, or a digital shaft encoder is used. One may ask whether such rugged devices are of any benefit for magnetohydrodynamic (MHD) flow measurements. As far as integral stationary flow properties in certain configurations are a matter, the answer is certainly yes.

Recently, both Tallbäck et al. [2] and Taniguchi et al. [3] successfully measured angular velocities in an electromagnetically driven rotary liquid metal flow. Inserting vanes similar to the left one depicted in Fig. 1 having sizes of almost that of the container diameter, these authors determined an integral value that corresponds, e.g., to the flow rate in a pipe.

The commercial availability of such small impeller-based vanes, as shown on the right-hand side for less than $ 400 including a data station, might suggest to perform semi-local measurements also. Regarding the performance of moving mechanical parts-based semi-local sensors, it is instructive to have a look at similar devices. Szekely et al [4] made use of a linear arrangement consisting of a spring loaded rod onto the head of which a $\phi = 19$ mm stainless steel disc was fastened. Although the displacement of the rod owing to the drag exerted on the disc was sensitively recorded by a linear voltage differential

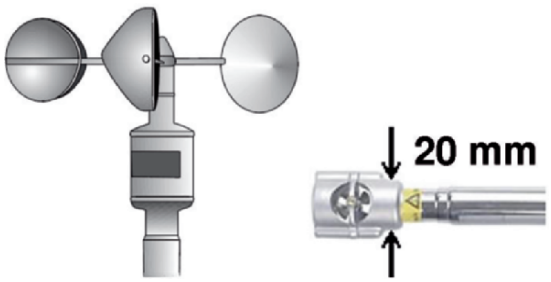

Fig. 1. Classical cup vane to determine wind speed (*left*) and miniaturised impeller-based vane probe (*right*)

transformer, the smallest velocity difference reported by the experimenters was 4 cm/s, and the smallest absolute value was 8 cm/s. For the suitability concerning the measurement of velocity fluctuations we quote the authors: "The inertia of the measuring system does not provide a great deal of insight into the structure of this turbulent flow." Force reaction probes comprising moving mechanical parts can be summarised to be restricted to time-averaged values at relatively high velocities and poor spatial resolution.

Another category of velocity probes makes use of directly measuring pressures, thus avoiding any moving mechanical part. The principle of operation of all these tubes is based on Bernoulli's law $p + \frac{\rho}{2}v^2 = p_0$, where p_0 denotes the total pressure, which is a constant, p the static pressure, and ρ and v the fluids density and velocity, respectively. In a stationary incompressible flow, the sum of the dynamic pressure $\frac{\rho}{2}v^2$ and p always results in the pressure within the resting fluid, which is that of the ambient atmosphere, plus the hydrostatic contribution ρgh of the fluid. Tube anemometers comprise basically a bend with one end directed in such a way that it faces the flow. As the kinetic energy is converted into potential one at the stagnation point, all tubes measure at least the total pressure p_0. Once the static pressure is known, the simpler Pitot tube allows the determination of the velocity according to Bernoulli's law. The static pressure p can only be determined accurately by measuring it in a manner such that the velocity pressure has no influence on the measurement at all. This is achieved by measuring it at right angle to the streamlines. The Prandtl tube sketched in Fig. 2 is an example of this, where p is determined through several static taps arranged circumferentially in the outer tube. A differential manometer thus allows for a direct measurement of the fluid velocity.

There exists not a huge number of research reports wherein Pitot and Prandtl tubes have been applied to liquid metal flows particularly addressing questions about sensitivity. From the few available it turns out that Pitot

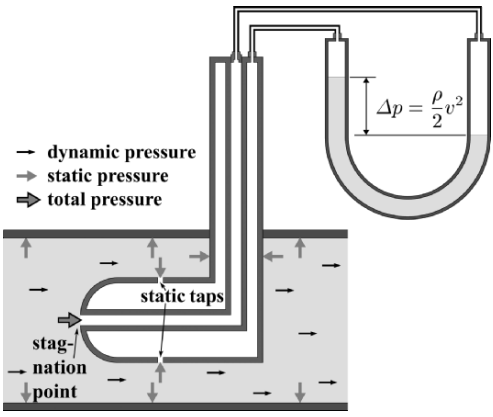

Fig. 2. Schematic diagram of a Prandtl tube

tubes are advantageous because they can be manufactured in smaller size. Typical outer diameters are in the range of a few millimetres. Moreau [5] points out that care has to be taken when magnetic fields are involved, a situation which is almost intrinsic to MHD experiments. Then, the stagnation pressure is not exactly equal to the fluid's loss of kinetic energy because of electromagnetic forces. It is estimated in [5] that this effect becomes significant for the smaller velocities of about 1 cm/s, which may be seen as the lower range of reliable operability of tube-based anemometers in liquid metals. Besides [5], for further reading see Branover et al. [6] and references therein.

It is obvious that this technique is not suitable for turbulence measurements if, e.g., a U-manometer is used as a pressure sensor owing to inertia of the fluid moving in the limbs. An attractive perspective of the method is offered by the availability of piezo-resistive pressure transducers. We successfully measured static pressure fluctuations in a 50 Hz AC electro-vortically driven flow through a ϕ =1 mm hole drilled into the chamber wall at sampling rates exceeding 1 kHz [7]. One may think about a Pitot tube consisting of a bent syringe and a piezo-transducer mounted at the other end. In [8], Pitot pressure surveys in a liquid metal atomization nozzle were reported, making use of a ϕ = 0.9 mm stainless steel tube. Operating also at the comparatively high rate of 1 kHz, the authors have been able to detect the transition from subsonic to supersonic flow regimes. It convincingly demonstrates the potential of tube-based anemometers.

With fibre flowmeters we return to the moving mechanical parts, but in a somewhat miniaturized variant and optical recording. In an early work, Griffiths and Nicol [9] mounted a single quartz fibre in a wall of a pipe in such a way that it protruded at a right angle to the flow direction. The deflection of the fibre tip was observed from the opposing side of the pipe by means of a travelling microscope. In an air experiment, velocities down to 10 cm/s were successfully recorded. Zhilin et al. [10] and Eckert et al. [11] constructed more complex sensors upon this principle, which were proven to work in liquid metals. A thin glass rod of several tens of μm in diameter was sealed into a thin-walled conical glass tube. The other end of this pointer was either blackened and brought into the light path where it led to absorption [10], or illuminated and observed by means of an endoscope [11]. Both techniques allowed for velocity resolution below 1 cm/s of two components. A remarkable feature of fibre sensors is the applicability to electro-vortical flows. Using the technique described in [11], Cramer et al. [7] determined the flow field in the comparable small volume of $2 \times 4 \times 2.5$ cm^3 throughflown by currents as high as several kiloamperes (kA) conveyed from a point source. Whereas the spatial resolution perpendicular to the sensor's axis was very high, the problem with the extended range of axial sensitivity was coped with by a mixed experimental–numerical approach. Based on bending moment theory, a numerical model of the probe was implemented predicting the integrated response of the sensor from a calculated flow field. These results were found to be in good agreement with the measurements.

2.2 Thermal anemometers

A wet finger in the air will detect the direction of the wind because a drop in temperature is felt on the surface facing the wind. Thermal anemometers act in a similar way, in that the passage of fluid takes heat away from a heated element at a rate dependent upon the velocity. This element, which is either a thin wire that can be made very short, or a metallic film on a quartz or ceramic substrate, is mounted at the end of a probe that can be inserted into the liquid under investigation. The mode of operation is either the change of electrical resistance at constant current, or the measurement of the current required to keep the resistance at a constant set point. Since the resistance will always be proportional to the temperature, the latter are frequently termed constant temperature anemometer. In practice, the resistance is measured or controlled by means of a Wheatstone bridge, one leg of which is the thermal probe.

Owing to their principle, the velocity readout of thermal probes seems instantaneous at first sight. However, even a very fine hot wire by itself cannot respond to changes in fluid velocity at frequencies above 500 Hz. By compensating for frequency lag with a non-linear amplifier this response can be increased to values exceeding 100 kHz. When compared with hot wires the cylindrical hot-film sensor, depicted in the upper right part of Fig. 3, has basically two advantages. A better frequency response is achieved because the sensitive part is distributed on the surface rather than on the entire cross section as with a wire. Secondly, the heat conduction to the supports (end losses) for a given length to diameter ratio are smaller due to the low thermal conductivity of the substrate material. A shorter sensing length thus can be used.

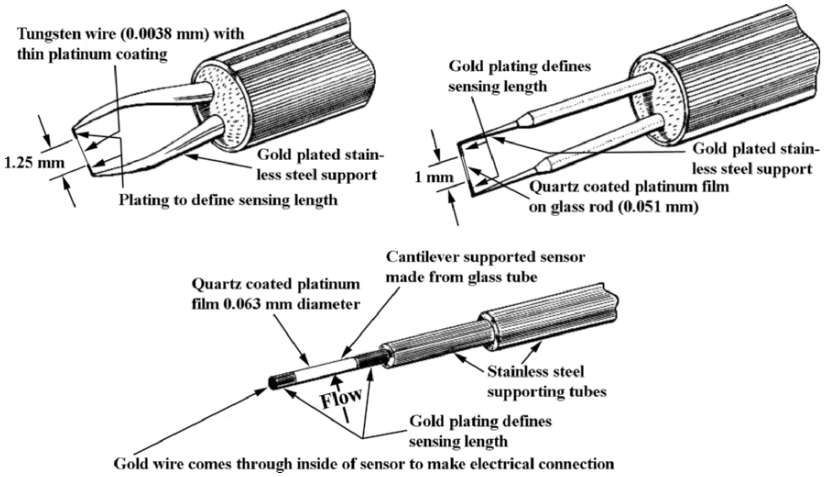

Fig. 3. Examples of commercially available hotwire (*top left*) and hotfilm (*top right* and *bottom*) probes. In particular, the lengths of the wire and the cantilever of the single-ended film sensor can be made very short

Hot-wire anemometers, employed mostly in gases by then, have been adopted for liquid metals in the 1960s. Sajben [12] reported on a system that was suitable in mercury at velocities from 1 to 12 cm/s. An improvement of this technique by Trakas et al. [13], also applied to a flow of mercury, revealed the capabilities of hot-film probes regarding velocity resolution. They were conditionally restricted upon principle to velocities of a few millimetre per second, which today may still be seen as the sensitivity threshold for an employment in liquid metals. Hot wire and film sensors are prone to fouling and deposition of debris and oxides, which change the transport properties of heat. Because they are thermal devices, it is important to compensate carefully for variations in ambient temperature and pressure. In particular, when applied in the low Prandtl number liquid metals, the high ratio between diffusive and convective heat transport leads to a significant decrease of resolution. All these drawbacks render the use of these thermal sensors in liquid metals somewhat inconvenient if not even tedious [14, 15]. For a typical MHD application, Robinson and Larsson [16] is referred to, who determined the mean velocity field in a flow driven by a rotating magnetic field.

Quick response is one of the prerequisites for turbulence measurements. Further, this measuring task puts a severe restriction on the size of the sensor in order to resolve all scales of potentially significant vortices. Being not restricted to thermal probes, this means that the finite extension of the sensitive zone acts as a lowpass filter with respect to the time domain. Because thermal sensors fulfill both suppositions, they have been intensively used in the study of turbulence. To quote a few, Alemany et al. [17] is referred to, who investigated the influence of a DC magnetic field on the flow of mercury created by a moving grid with a hot-film sensor attached behind the grid. Recently, Petrović et al. [18] reported on the accuracy of turbulence measurements by hot wires. The article quotes a variety of modern studies devoted to hot wires and somehow addresses the question about their perspectives, in particular of such ones having up to 12 sensing wires.

2.3 Potential difference probes

Often these probes are also named the conductive anemometers. This may be due to the fact that the sensing wires of the probe are in electrical contact with the conducting medium. The basic principle consists in measuring a voltage drop $\Delta\phi$ induced by a magnetic field $\mathbf{B}$ across its wire spacing Δl according to Ohm's law: $\mathbf{j} = \sigma(E + \mathbf{u} \times \mathbf{B})$. In the absence of electric currents $\mathbf{j}$, the electric field strength E, expressed by a finite difference of the potential $E \approx \Delta\phi/\Delta l$ for sufficiently small sensor dimensions, is independent of the electrical conductivity σ, and is linearly related to the velocity $\mathbf{u}$. Determination of fluid velocities via this electromotive force (e.m.f.) dates back to Faraday [19]. He had tried vainly to measure the voltage induced across the river Thames by the motion of the water in the earth's magnetic field. Kolin [20] proposed to use a probe consisting of two wires, insulated except at

the tip, with a separation of the wire tips in the order of a few thousandths of an inch. In an orthogonal arrangement with a homogeneous static measuring field, the potential difference induced between the wires should then be a direct measure of the corresponding velocity component.

The measuring magnetic field can be applied either globally over the entire melt volume, or locally confined to the wire tips. Again Kolin [21] was among the first who used also incorporated magnet probes. Equipped with a small electromagnet, the probe's sensitivity must have been poor. Ricou and Vives [22] reported on a feasible solution using rare-earth CORAMAG and ALNICO permanent magnets, the latter were even operable in aluminium melts. As any sensor immersed into the fluid poses an obstacle, the influence of which onto the flow increases with size, the question about how small a probe can be build becomes an important issue. From this point of view, the potential difference probes (PDP) using a globally applied field are seemingly advantageous because they essentially consist only of two wires. On the other hand, it is well known that static fields may damp the flow to be measured. Compared to a typical hot wire having $\phi = 1$ mm, the probes in [22] were several times larger. A globally applied field with the same strength as that acting in the incorporated probe in [22] certainly influences the flow significantly. Because the sensitivity of PDPs is determined by the product of field strength and wire spacing, we are concerned here with the usual compromise inherent to every measurement task. Without dismissing sensitivity, which was about 1 cm/s minimum velocity at a stated by the authors of [22] resolution of 1 mm/s, Weissenfluh [23] constructed PDPs having $\phi \approx 1$ mm. At this stage it may be summarized that PDPs compare well to hot wires regarding performance. The drawback that they are not suited in many configurations owing to the presence of electric currents (see [24]) is compensated by the ease of use.

Similar to thermal sensors, PDPs have been thoroughly employed for the measurement of mean velocities down to their resolution of around 1 mm/s [25, 26], and to determine turbulence characteristics of fast flows [27, 28]. An advantage of PDPs is the utilization in those cases where a strong magnetic field is intrinsic to the problem. This branch of investigations comprises basic research, e.g., two–dimensional (2D) turbulence [29,30], as well as applications in fusion technology [31]. In this context, one particular technique is worth noting. When the fluid flow becomes quasi-2D in a sufficiently high magnetic field, the electric potential does not vary considerably, neither in the core nor in the Hartmann layers. Davoust et al. [32] and Messadek and Moreau [33] acquired velocities non-invasively at the Hartmann wall by means of electrodes mounted in the wall. These measurements yielded to a good approximation the core velocity values in planes perpendicular to the applied field. Besides observing local fluid velocities in an ideally isothermal flow, adding at least a third electrode allows to account for temperature effects produced by thermoelectricity (Seebeck effect). It depends on the particular choice of geometry, the number of electrodes, and the materials thereof whether the fluid velocity

is measurable without thermoelectric disturbances or the temperature can be measured in addition. Examples for such combined probes are to be found in [23, 31, 32].

Summarizing so far it becomes obvious that: (i) further miniaturization of incorporated magnet PDPs below 1 mm will lead to a serious decrease in sensitivity; (ii) the use of a globally applied field with the same strength of that locally acting in incorporated PDPs is often unacceptable because of the influence on the flow; (iii) any tip spacing $\Delta l > 1$ mm does hardly allow for turbulence measurements, according to Bolonev et al. [34], who determined experimentally the influence of Δl on the transfer function, which quantifies the above-mentioned spatial integration leading to a lowpass filtering in the time domain; (iv) a significant increase in sensitivity of e.m.f.-based measurements can consequently be achieved only by an as good as possible noise – and disturbance – free set-up of the electronic data acquisition system.

At least since the work of Remenieras and Hermant [35] tackling the problem of inductive transients and noise in e.m.f.-based velocity measurements, it became obvious that a fully differential-ended amplifier chain is mandatory despite of the low impedance source of the probe. Using state-of-the-art instrumentation with high impedance coupling between amplifier stages and meticulously avoiding systematic disturbances such as thermoelectricity, we have been able to extend the sensitivity of mean velocity measurements to 10^{-2} mm/s for a $\Delta l = 1$ mm probe. From the calibration curve in Fig. 4 it is seen that voltages less than 1 nV had to be acquired reliably. As sensitivity, resolution, and bandwidth are always a compromise, the performance of the measuring chain allowed the determination of velocity fluctuations in a flow driven by a rotating magnetic field commencing slightly above the threshold of linear stability. This corresponded to a mean velocity of a little less than 3 cm/s, over a wide range of the Taylor number. Figure 5 demonstrates that it

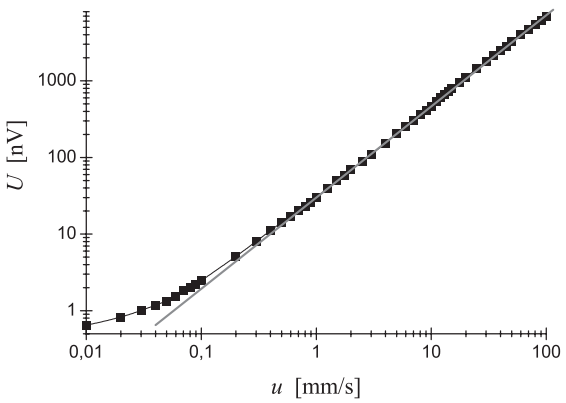

Fig. 4. Calibration curve of an incorporated magnet PDP using highly sensitive analog instrumentation. The probe response was non-linear below 1 mm/s

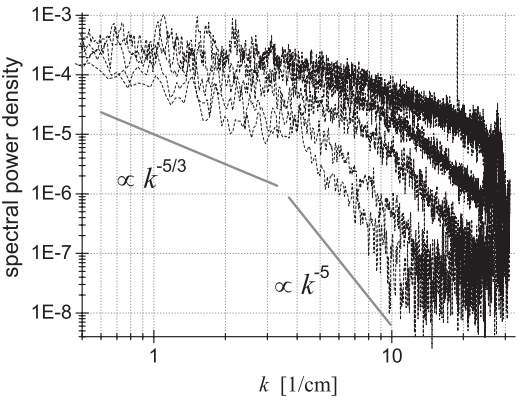

Fig. 5. Power spectra of velocity fluctuations in a flow driven by a rotating magnetic field from slightly above the linear stability threshold (steepest slope of inertial range) spanning a range of factor 15 in the governing parameter [36]

was always possible to resolve all scales of wavelengths. A detailed description of the experiment and the electronics can be found in Cramer et al. [36].

3 Non-invasive techniques

3.1 Ultrasonic methods

Ultrasonic methods are non-invasive, but not fully contactless. A continuous acoustic path from the ultrasonic transducer to the liquid under investigation is required for transmission of the ultrasonic wave into the flow region and for reception of the measuring signal.

Two common principles are known to apply ultrasound for measurements of fluid velocities: the ultrasonic Doppler and the transit time, also called the time-of-flight technique. The operating mode of ultrasonic flowmeters by the transit-time method is based on two sequential measurements: an ultrasonic pulse is sent between two transducers upstream and downstream through the liquid. The run-time difference between downstream acceleration and upstream deceleration delivers the averaged velocity. To obtain local information about the flow field, Johnson et al. [37] proposed a method to measure three-dimensional (3D) flows by transmitting and receiving ultrasonic beams along a multitude of lines. The arrangement is that each volume element is traversed by a set of lines having components in each direction for which flow components are to be reconstructed. Each propagation time measurement of the ultrasonic wave is an integral of a function of sound speed and fluid velocity along the particular line leading to a set of integral equations, which have to be inverted to obtain the unknown fluid velocity vector field.

A more promising way to measure local velocities is offered by the ultrasound Doppler method, often called ultrasound Doppler velocimetry (UDV) or ultrasonic velocity profile (UVP) monitor. The origin of this technique can be retraced to the medical branch [38]. Owing to the pioneering work of Takeda [39, 40] it has also been established in physics and fluids engineering. The measuring principle is based on the pulsed echo technique. Ultrasound pulses of a few cycles are emitted from the transducer and travel along the measuring line. If such a pulse hits microparticles suspended in the liquid, a part of the ultrasonic energy is scattered. It can be received using a second transducer or by the same transducer working in the listening mode between two emissions. In the majority of cases the second variant is realized. The entire information of the velocity profile along the ultrasonic beam is contained in the echo. If the sound velocity of the liquid is known, the spatial position along the measuring line can be determined from the detected time delay between the burst emission and its reception. The movement of an ensemble of scattering particles inside the measuring volume will result in a small time shift of the signal structure between two consecutive bursts. The velocity is obtained from a correlation analysis between consecutive bursts. The measuring principle is sketched in Fig. 6. Owing to the Nyquist theorem, the product of measurable maximum velocity and penetration depth is limited by the sound velocity and the ultrasonic frequency. For a more detailed description of the basics of the measuring principle the reader is referred to Takeda [40].

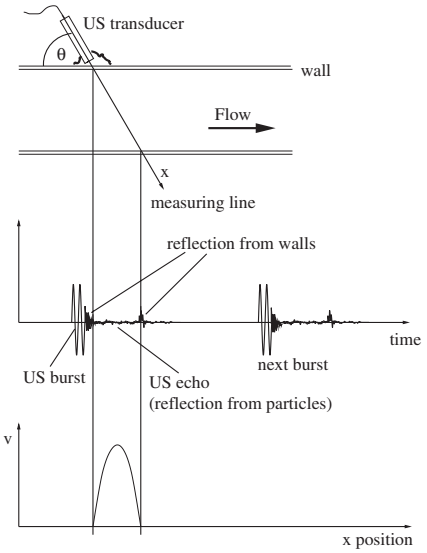

Fig. 6. UDV-measuring principle shown for a channel flow

We want to focus here on a few problems arising especially with the application of UDV to liquid metal flows, namely the load of the sensors due to high temperatures and the chemical aggressiveness of the melt, the transmission of the ultrasonic waves through container walls, the acoustic coupling between the transducer, the wall and the melt, as well as the allocation of suitable reflecting particles inside the liquid metal. The feasibility of velocity profile measurements in liquid metals using UDV has been demonstrated for the first time by Takeda [41], who measured velocity profiles in a T-tube filled with mercury at room temperature. Further successful applications have been published by Brito et al. [42] for liquid gallium and by Eckert and Gerbeth [43] for liquid sodium at a temperature of about 150°C. In many applications the ultrasonic transducer cannot be brought into direct contact with the liquid metal. The ultrasonic methods also allow measurements through the container wall as shown in Fig. 7 for the case of a channel flow. However, one has to take into account that any additional interface in the ultrasonic path diminishes the energy of the ultrasonic beam. One reason for such losses might be a mismatch between the acoustic impedances Z of the wall material and the liquid metal, which is rather pronounced for liquid sodium ($Z_{Na} = 2 \times 10^6$ Ns/m^3) flowing inside a channel of stainless steel ($Z_{SS} = 4.5 \times 10^7$ Ns/m^3). In this case, the transmission of a sufficient amount of ultrasonic energy through the wall can only be assured if the wall thickness meets almost exactly a multiple of half the wavelength of the ultrasonic wave in the wall material [43]. Another issue is the wetting at the inner wall. The occurrence of thin gas or oxide layers impedes the passover of the ultrasonic wave into the liquid metal. Brito et al. [42] performed UDV measurements in a vortex of liquid gallium confined in a cylindrical vessel made from different materials (polycarbonate,

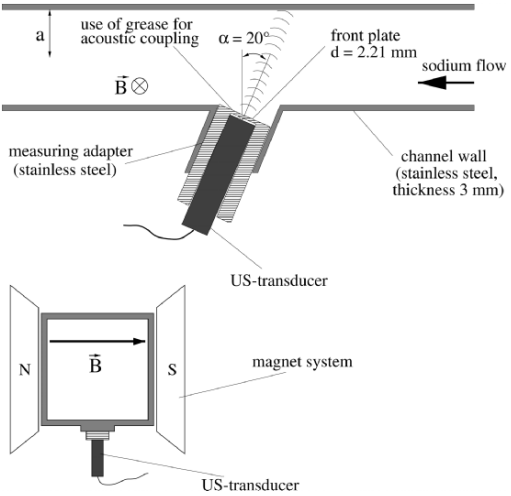

Fig. 7. UDV measurements for a sodium channel flow [43]

nylon, copper). The authors observed a continuous deterioration of the signal quality with progressing time of measurements. This phenomenon was related to oxide films developing at the inner cylinder wall. To prevent adherence of oxides at the wall the authors proposed a special coating with a cataphoretic film. Experiences gained with stainless steel and liquid sodium [43] confirm that oxide layers at the contact surface must be eliminated to guarantee a low-loss transmission of the ultrasonic wave.

The conventional piezoelectric transducers using lead zirconate titanate (PZT)-based materials are usually restricted to a temperature range below 200°C. Other piezoelectric materials with higher Curie temperatures like $GaPO_4$ or $LiNbO_3$ can work up to temperatures of 650°C or 900°C, respectively. Such sensors have already been used for fluid level detectors in liquid metal fast breeder reactors [44]. However, the piezoelectric coupling factor of the heat-resistant piezoelectric materials is by a factor of about 5 less than that for standard materials. This leads to a worse signal-to-noise ratio and, thus, results in a sensitivity, which is insufficient for UDV measurements. The application of acoustic wave guides as a buffer between the hot liquid and the piezoelectric elements is another approach to elude the temperature restriction of 200°C. Different types of acoustic waveguides, consisting in the simplest version of a solid cylinder of heat-resistant material, have already been applied to extend the working range of ultrasonic flowmeters towards higher temperatures [45, 46]. The structure of waveguides for Doppler shift measurements appears to be more sophisticated because a monomode propagation of the ultrasonic wave inside the waveguide is required. This results in a restriction for the thickness of the waveguide structures. Gelles [47] demonstrated the basic features of a fiber-acoustic waveguide consisting of a bundle of cylindrical fibres. Eckert et al. [48] presented a waveguide made of a stainless steel foil with a thickness of 0.125 mm as shown in Fig. 8. The thinner the waveguide structures, the higher the emission frequencies can be applied, and the lower the velocities can be measured. The operability of such steel waveguides has already been demonstrated in CuSn and aluminium at temperatures up to 750°C [48, 49].

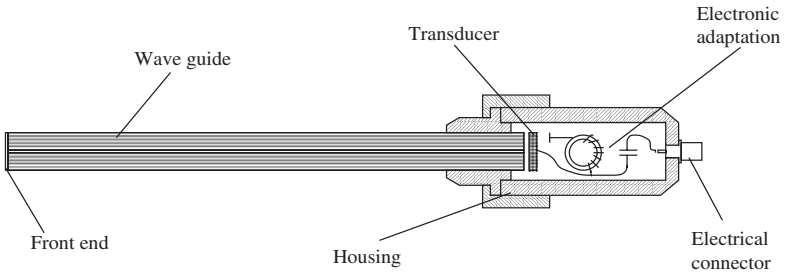

Fig. 8. Ultrasonic sensor with integrated acoustic waveguide for measurements in hot metallic melts

Doppler devices require the presence of scattering objects inside the fluid. Artificial or natural particles, gas bubbles, or fluctuations in density can serve for this purpose. There is a lack of quantitative studies in liquid metals focusing on the dependence of signal properties on parameters, such as concentration, morphology (e.g., size, shape) and acoustic properties of the suspended reflectors. The signal quality depends on the optimal particle concentration. Though low concentration does not disturb the propagation of the ultrasonic wave significantly, the sensitivity of the measurements deteriorates. On the other hand, high concentration improves the sensitivity but increases the attenuation and, in turn, limits the depth of the measurement. Scattering particles to be added to the flow should match the fluid density to avoid a slip between the fluid and particle motion and to guarantee homogeneous distribution in the entire fluid volume. Moreover, the particles need to be wetted by the liquid to avoid agglomeration effects. It is obviously favourable to work solely with natural impurities usually existent in metallic melts with a common, technical purity standard. Noble liquid metals, such as mercury, contain an insignificant amount of natural tracers, whereas, for instance, in liquid gallium or gallium alloys, a distinct oxidation cannot be avoided with reasonable effort. Here, the situation could arise that the UDV measurements might be complicated by too many tracers inside the measuring volume [42, 50].

Another essential point of interest is the question with respect to the capability of the UDV technique for analysing turbulent velocity fluctuations. In the past, electromagnetic potential probes were used in MHD turbulence research to record local time series, and to calculate the frequency power spectrum [29]. Because of the statistical character of the measuring principle the UDV method is inferior regarding the time resolution of both measuring techniques. A number of US bursts have to be superposed in order to get a reliable velocity signal. Depending on the distinct experimental conditions this requirement typically leads to time resolution of between 10 and 100 ms. On the other hand, the UDV technique delivers the local velocity simultaneously at different locations along one measuring line. Usually, the turbulent energy $E(k)$ is derived from the frequency power spectrum $P(f)$ by employing Taylor's hypothesis. In many applications, for instance, the electromagnetic stirring in confined geometries, this assumption becomes questionable because a clearly dominating mean flow, which moves a frozen turbulent structure, does not exist. Regardless of the limitations in time resolution, the UDV method allows a direct calculation of the velocity structure functions, and therefore provides information about the scaling properties of the flow. Takeda [51,52] studied the transition from laminar flow to turbulent in a rotating Taylor–Couette system by measuring the spatiotemporal velocity field. To analyse the velocity structure quantitatively he applied spatial and temporal Fourier transform and orthogonal decomposition techniques. Related studies on thermal turbulence in mercury have recently been published by Mashiko et al. [53] and Tsuji et al. [54].

The amount of publications dealing with UDV measurements in liquid metal flows is still manageable. This measurement technique can provide valuable insight in miscellaneous flow situations, occurring for instance, during electromagnetic stirring [50], during solidification of metallic alloys [55], inside a mercury target for a spallation source [56] or in MHD two-phase flows [57].

3.2 Radioscopic techniques

Visible light cannot be used for flow visualization in metallic melts because penetration of macroscopic metallic layers requires photon energies of at least 10 keV. On the other hand, radioscopic techniques working with short-wavelength radiation, such as x-rays or nuclear radiation, have been employed for in situ investigations of kinetics and morphology of solid–liquid interfaces during solidification. Information about the flow pattern can also be obtained. Szekely [58] determined the turbulent diffusivity in liquid steel using radioactive tracers. For this reason he introduced a capsule containing radioactive gold into the centre of the bath. Samples of the steel were periodically taken out at certain positions and the radioactive content was measured. Stewart and Weinberg [59] introduced radioactive material into liquid tin to delineate the flow pattern. After a certain period of time, the system was rapidly quenched in order to freeze the tracer position. The tracer profile was taken as representative of the flow pattern. Obviously, these first realizations have to be considered as fairly crude and by no means non-invasive. An in situ monitoring of the tracer movement in the melt is necessary. Kakimoto et al. [60] report about a direct observation of the flow structure in molten silicon by x-ray radiography. The authors developed a multilayered tracer consisting of a small tungsten cylinder in the sensor. The tungsten was covered by layers of SiO_2 and carbon to adjust the density to that of silicon and to wet the tracer by the molten silicon. X-rays penetrating the silicon pool during the process were detected by an image intensifier. Because of the much larger absorption coefficient the momentary position of the singular tungsten particle can be followed by the visualization system allowing the reconstruction of the particle trajectory.

Another approach is the visualization of the density field as proposed by Koster et al. [61–64]. X-ray absorption within material depends on the mass attenuation coefficient, fluid density, and the material thickness in the direction of the penetrating radiation. If the density is altered by temperature, the method provides a temperature field visualization being related to the velocity field in natural convection. This radioscopic technique was tested with a natural convection benchmark study in liquid gallium [63]. The weak dependence of the density on temperature in metallic melts requires additional efforts, for instance, to carefully avoid beam scattering in the environment, to achieve excellent resolution of the radioscopic system. Koster et al. [63] published a highest resolution in detection of local density changes of 0.02%. A very recent development is the application of high frame-rate neutron radiography

to investigate liquid metal two-phase flows. Saito et al. [65, 66] performed experiments using the JRR-3M nuclear research reactor providing high neutron fluxes. Gold–cadmium particles were added to a lead–bismuth melt, and 2D velocity fields were reconstructed using particle tracking velocimetry.

3.3 Flow tomography from measurements of the induced magnetic field

Magnetoencephalography (MEG) is well established in the medical branch as a convenient method to study the brain function and diseases, such as epilepsy [67]. Low electric currents flowing inside the neurons generate magnetic fields which can be measured outside the body, thus providing a remarkably accurate representation of the local brain activity. Is it conceivable to use a similar principle for flow measurements? To answer this question, let us consider an electrically conducting liquid flowing within a certain volume. By imposing an external magnetic field, such an unknown flow field will generate a distribution of induced currents inside the liquid and thereby an induced magnetic field. The latter is present inside, as well as outside of the melt volume. The structure of the induced field obviously contains information about the flow. A reliable interpretation of this information would provide a fully contactless method to determine 3D velocity fields. The strength of the applied fields must be sufficiently weak, so that the flow to be measured is not influenced. However, this measuring principle can also be applied in cases where stronger magnetic fields are already present in the process under consideration, for instance, in continuous casting with an electromagnetic brake or in single crystal growth processes.

The first attempt to utilize this principle for flow measurements was undertaken by Köhler et al. [68]. The authors applied a few local sensors to detect the flow velocity of liquid steel in the mould in close vicinity to the sensor position. The sensors consisting of permanent magnets and highly sensitive magnetic field detectors were positioned close to the wall of the mould. Because of difficulties regarding the sensor calibration, the velocity information was obtained by correlating the output signal of two adjacent sensors. The question is obvious whether a complete reconstruction of the velocity field can be realized using a sufficient number of magnetic field sensors around the fluid volume to be measured. Stefani et al. [69] showed that the sole measurement of the induced magnetic field, even using numerous sensors, cannot deliver a unique solution of the problem as long as the electrical potential at the surface of the fluid volume is not taken into account. The determination of the electric potential requires a set of electrodes at the fluid surface implicating that the principle thus becomes less attractive for hot and aggressive fluids or for facilities where the fluid boundary is not accessible owing to technological reasons. The problem can be solved by subsequent application of various external magnetic fields to the same flow field [70]. The imposition of two orthogonal magnetic fields represents a certain minimum configuration

for a fully contactless flow tomography. An experimental demonstration of a contactless inductive flow tomography (CIFT) has been reported by Stefani et al. [71]. The scheme of this experiment is shown in Fig. 9.

A cylindrical vessel with an aspect ratio close to 1 contains about 4.5 l of the eutectic alloy GaInSn. A propeller forces a flow inside the vessel up to maximum velocities of 1 m/s, which corresponds to a magnetic Reynolds number $R_m \approx 0.4$. Two pairs of Helmholtz coils consecutively produce axial and transverse magnetic fields. The induced magnetic fields are measured by 49 Hall sensors at different positions around the vessel. The main problem of the method is that the values of the induced magnetic fields are some orders of magnitude lower than the applied field. The authors let the propeller rotate in both directions, resulting either in an upward or in a downward pumping with different flow structures. Whereas the downward pumping produces both a main poloidal roll and a toroidal motion, the latter one is, to a large extent, inhibited by guiding blades for the upwards pumping. The CIFT technique was able to discriminate between those different flow patterns [71]. By comparing these measurements with the UDV technique it was further shown that not only the structure, but also the range of the velocity scale was correctly reproduced, see the right part of Fig. 9.

A particular advantage of CIFT is the transient resolution of the full 3D flow structure in steps of several seconds. Hence, slowly changing flow fields in various processes can be traced in time. Further developments of this measuring principle will use also AC magnetic fields to improve the depth resolution of the determined velocity field.

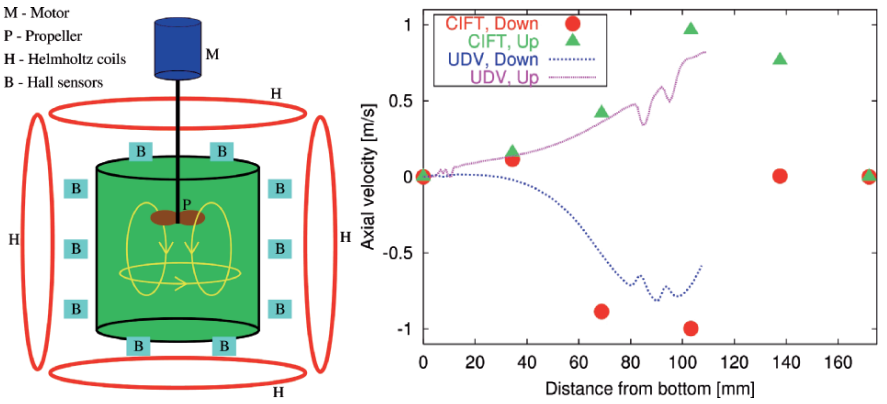

Fig. 9. Scheme of the CIFT demonstration experiment (*left*), and comparison of CIFT and UDV velocity measurements (*right*) for the axial velocities along the central vertical axis of the cylinder (UDV measurements are only shown up to the propeller position, whereafter they become unreliable) [71]

References

1. Brusey BW, Brussiere JF, Dubois M, Moreau A (eds) (1999) Advanced Sensors for Metal Processing. Canadian Institute of Mining, Metallurgy and Petroleum, Montreal
2. Tallbäck GR, Lavers JD, Beitelman LS (2003) Simulation and measurement of EMS induced fluid flow in billet/bloom casting systems. In: Asai S, Fautrelle Y, Gillon P (eds) Proceedings of the 4^{th} International Symposium on Electromagnetic Processing of Materials, Lyon, France, pp 154–159
3. Taniguchi S, Maitake K, Okubo M, Ando T, Ueno K (2003) Rotary stirring of liquid metal without free surface deformation by combination of rotational and vertical traveling magnetic fields. ibid, pp 339–343
4. Szekely J, Chang CW, Ryan RE (1977) The measurement and prediction of the melt velocities in a turbulent, electromagnetically driven recirculating low melting alloy system. Metal Trans 8B:333–338
5. Moreau R (1978) Local and instantaneous measurements in liquid metal MHD. Proc Dynamic Flow Conf, pp 65–79
6. Branover H, Gelfgat YM, Tsinober AB, Shtern AB, Shcherbinin EV (1966) The application of Pitot and Prandtl tubes in magnetohydrodynamic experiments. Magnetohydrodynamics 2:55–58
7. Cramer A, Gerbeth G, Terhoeven P, Krätzschmar A (2004) Fluid velocity measurements in electro–vortical flows. Mat and Manufact Processes 19:665–678
8. Mates SP, Settles GS (1995) A flow visualization study of the gas dynamics of liquid metal atomization nozzles. In: Proceedings of the International Conference on Powder Metallurgy and Particulate Materials, Seattle, USA
9. Griffiths RT, Nicol AA (1965) A fibre flowmeter suitable for very low flow rates. J Sci Instrum 42:797–799
10. Zhilin VG, Zvyagin KV, Ivochkin YP, Oksman AA (1989) Diagnostics of liquid metal flows using fibre-optic velocity sensor. In: Lielpeteris M, Moreau R (eds) Liquid Metal Magnetohydrodynamics, Kluwer Academic, Dordrecht, 373–379
11. Eckert S, Gerbeth G, Witke W (2000) A new mechano–optical technique to measure local velocities in opaque fluids. Flow Meas Instrum 11:71–78
12. Sajben M (1965) Hot wire anemometer in liquid mercury. Rev Sci Instrum 36:945–953
13. Trakas C, Tabeling P, Chabrerie JP (1983) Low–velocity calibration of hot–film sensors in mercury. J Phys E: Sci Instrum 16:568–570
14. Argyropoulos SA (2000) Measuring velocity in high–temperature liquid metals: a review. Skand J Metallurgy 30:273–285
15. Reed CB, Picologlou BF, Dauzvardis PV, Bailey JL (1986) Techniques for measurement of velocity in liquid–metal MHD flows. Fusion Technol 10:813–821
16. Robinson T, Larsson K (1973) An experimental investigation of a magnetically driven rotating liquid-metal flow. J Fluid Mech 60:641–664
17. Alemany A, Moreau R, Sulem PL, Frisch U (1979) Influence of an external magnetic field on homogeneous turbulence. J de Méchanique 18:277–313
18. Petrović DV, Vukoslavčević PV, Wallace JM (2003) The accuracy of turbulent velocity component measurements by multi–sensor hot wire probes: a new approach to an old problem. Exp Fluids 34:130–139
19. Faraday M (1832) Experimental researches in electricity – second series (Bakerian lecture). Phil Trans Roy Soc 175:197–244

20. Kolin A (1943) Electromagnetic method for the determination of velocity distribution in fluid flow. Phys Rev 63:218–219
21. Kolin A (1944) Electromagnetic velometry. I. A method for the determination of fluid velocity distribution in space and time. J Appl Phys 15:150–164
22. Ricou R, Vives C (1982) Local velocity and mass transfer measurements in molten metals using an incorporated probe. Int J Heat Mass Transfer 25:1579–1588
23. Weissenfluh T (1985) Probes for local velocity and temperature measurements in liquid metal flow. Int J Heat Mass Transfer 28:1563–1574
24. Tsinober A, Kit E, Teitel M (1987) On the relevance of the potential–difference method for turbulence measurements. J Fluid Mech 175:447–461
25. Gelfgat YM, Gelfgat AY (2004) Experimental and numerical study of rotating magnetic field driven flow in cylindrical enclosures with different aspect ratios. Magnetohydrodynamics 40:147–160
26. Barz RU, Gerbeth G, Wunderwald U, Buhrig E, Gelfgat YM (1997) Modelling of the isothermal melt flow due to rotating magnetic fields in crystal growth. J Cryst Growth 180:410–421
27. Grossman LM, Charwat AF (1952) The measurement of turbulent velocity fluctuations by the method of magnetic induction. Rev Sci Instrum 23:741–747
28. Bojarevičs A, Bojarevičs V, Gelfgat YM, Pericleous K (1999) Liquid metal turbulent flow dynamics in a cylindrical container with free surface: experiment and numerical analysis. Magnetohydrodynamics 35:258–277
29. Kolesnikov YB, Tsinober AB (1972) Two–dimensional flow behind a cylinder. Magnetohydrodynamics 8:300–307
30. Eckert S, Gerbeth G, Witke W, Langenbrunner H (2001) MHD turbulence measurements in a sodium channel flow exposed to a transverse magnetic field. Int J Heat Fluid Flow 22:358–364
31. Burr U, Barleon L, Müller U, Tsinober AB (2000) Turbulent transport of momentum and heat in magnetoydrodynamic rectangular duct flow with strong sidewall jets. J Fluid Mech 406:247–279
32. Davoust L, Cowley MD, Moreau R, Bolcato R (1999) Buoyancy–driven convection with a uniform magnetic field. Part 2. Experimental investigation. J Fluid Mech 400:59–90
33. Messadek K, Moreau R (2002) An experimental investigation of MHD quasi two-dimensional turbulent shear flows. J Fluid Mech 456:137–159
34. Bolonev N, Charenko A, Eidelmann A (1976) About the correction of turbulence spectra measured using conductivity anemometers. Ing Phys J 2:243–247 (in Russian)
35. Remenieras G, Hermant C (1954) Mesure électromagnétique des vitesses dans les liquides. Houille Blanche 9:732–746
36. Cramer A, Varshney K, Gundrum T, Gerbeth G (2006) Experimental study on the sensitivity and accuracy of electric potential local flow measurements. Flow Meas Instrum 17:1–11
37. Johnson SA, Greenleaf JF, Tanaka M, Flandro G (1977) Reconstructing three-dimensional temperature and fluid velocity vector fields from acoustic transmission measurements. ISA Trans 16:3–15
38. Atkinson P (1976) A fundamental interpretation of ultrasonic Doppler velocimeters. Ultrasound Med Biol 2:107–111
39. Takeda Y (1986) Velocity profile measurement by ultrasound Doppler shift method. Int J Heat Fluid Flow 7:313–318

40. Takeda Y (1991) Development of an ultrasound velocity profile monitor. Nucl Eng Design 126:277–284
41. Takeda Y (1987) Measurement of velocity profile of mercury flow by ultrasound Doppler shift method. Nucl Technol 79:120–124
42. Brito D, Nataf H-C, Cardin P, Aubert J, Masson JP (2001) Ultrasonic Doppler velocimetry in liquid gallium. Exp Fluids 31:653–663
43. Eckert S, Gerbeth G (2002) Velocity measurements in liquid sodium by means of ultrasound Doppler velocimetry. Exp Fluids 32:542–546
44. Boehmer LS, Smith RW (1976) Ultrasonic instrument for continuous measurement of sodium levels in fast breeder reactors. IEEE Trans Nucl Sci 23:359–362
45. Liu Y, Lynnworth LC, Zimmerman MA (1998) Buffer waveguides for flow measurement in hot fluids. Ultrasonics 36:305–315
46. Jen C-K, Legoux J-G, Parent L (2000) Experimental evaluation of clad metallic buffer rods for high temperature ultrasonic measurements. NDT&E In 33:145–153
47. Gelles IL (1966) Optical-fiber ultrasonic delay lines. J Acoust Soc Am 39:1111–1119
48. Eckert S, Gerbeth G, Melnikov VI (2003) Velocity measurements at high temperatures by ultrasound Doppler velocimetry using an acoustic wave guide. Exp Fluids 35:381–388
49. Eckert S, Gerbeth G, Gundrum T, Stefani F (2005) Velocity measurements in metallic melts. In: Proceedings of 2005 ASME FED Summer Meeting, FEDSM2005–77089
50. Cramer A, Zhang C, Eckert S (2004) Local flow structures in liquid metals measured by ultrasonic Doppler velocimetry. Flow Meas Instrum 15:145–153
51. Takeda Y (1999) Quasi-periodic state and transition to turbulence in a rotating Couette system. J Fluid Mech 389: 81–99
52. Takeda Y, Fischer WE, Sakakibara J (1993) Measurement of energy spectral density of a flow in a rotating Couette system. Phys Rev Lett 70:3569–3571
53. Mashiko T, Tsuji Y, Mizuno T, Sano M (2004) Instantaneous measurement of velocity fields in developed thermal turbulence in mercury. Phys Rev E 69:036306
54. Tsuji Y, Mizuno T, Mashiko T, Sano M (2005) Mean wind in convective turbulence of mercury. Phys Rev Lett 94:034501
55. Eckert S, Willers B, Gerbeth G (2005) Measurements of the bulk velocity during solidification of metallic alloys. Metall Mater Trans A 36:267–270
56. Takeda Y, Kikura H, Bauer G (1998) Flow measurement in a SINQ mockup target using mercury. In: Proceedings of 1998 ASME FED Summer Meeting, FEDSM98-5057
57. Zhang C, Eckert S, Gerbeth G (2005) Experimental study of a single bubble motion in a liquid metal column exposed to a DC magnetic field. Int J Multiphase Flow 31:824–842
58. Szekely J (1964) Experimental study of the rate of metal mixing in an open-hearth furnace. Journal ISIJ 202:505–508
59. Stewart MJ, Weinberg F (1972) Fluid flow in liquid metals. Experimental observations. J Cryst Growth 12:228–238
60. Kakimoto K, Eguchi M, Watanabe H, Hibiya T (1988) Direct observation by X-ray radiography of convection of molten silicon in the Czochralski growth method. J Cryst Growth 88:365–370

61. Campbell TA, Koster JN (1994) Visualization of liquid/solid interface morphologies in gallium subject to natural convection. J Cryst Growth 140:414–425
62. Campbell TA, Koster JN (1995) Radioscopic visualization of Indium Antimonide growth by the vertical Bridgman-Stockbarger technique. J Cryst Growth 147:408–410
63. Koster JN, Seidel T, Derebail R (1997) A radioscopic technique to study convective fluid dynamics in opaque liquid metals. J Fluid Mech 343:29–41
64. Derebail R, Koster JN (1998) Visualization study of melting and solidification in convecting hypoeutectic Ga-In alloy. Int J Heat Mass Transfer 41:2537–2548
65. Saito Y, Mishima K, Tobita Y, Suzuki T, Matsubayashi M (2005) Measurements of liquid-metal two-phase flow by using neutron radiography and electrical conductivity probe. Exp Therm Fluid Sci 29:323–330
66. Saito Y, Mishima K, Tobita Y, Suzuki T, Matsubayashi M, Lim IC, Cha JE (2005) Application of high frame-rate neutron radiography to liquid-metal two-phase flow research. Nucl Instrum Meth Phys Res A 542:168–174
67. Hämäläinen M, Hari R, Ilmoniemi RJ, Knuutila J, Lounasmaa OV (1993) Magnetoencephalography – theory, instrumentation, and applications to noninvasive studies of the working human brain. Rev Mod Phys 65:413–497
68. Köhler KU, Andrzejewski P, Julius E, Haubrich H (1994) Measurements of steel flow in the mould. In: Asai S (ed) Proceedings of International Symposium on Electromagnetic Processing of Materials, Nagoya, Japan, pp 344–349
69. Stefani F, Gerbeth G (1999) Velocity reconstruction in conducting fluids from magnetic field and electric potential measurements. Inverse Problems 15:771–786
70. Stefani F, Gerbeth G (2000) A contactless method for velocity reconstruction in electrically conducting fluids. Meas Sci Technol 11:758–765
71. Stefani F, Gundrum T, Gerbeth G (2004) Contactless inductive flow tomography. Phys Rev E 70:056306